Investigation into microdefects and corrosion resistance of nickel-titanium shape memory alloy using electrical discharge coating process

Ahmad Fairuz Mansor [a, *], Azwan Iskandar Azmi [a, *], Sikiru Oluwarotimi Ismail [b]

[a] *Faculty of Mechanical Engineering & Technology, Universiti Malaysia Perlis, Pauh Putra Campus, 02600 Arau, Perlis, Malaysia*

[b] *Department of Engineering, Centre for Engineering Research, University of Hertfordshire, Hatfield AL10 9AB, England, United Kingdom*

[*]Corresponding authors: fairuzmansor@unimap.edu.my, azwaniskandar@unimap.edu.my

Abstract

Nickel-titanium shape memory alloy is a novel material with outstanding properties suitable for biomedical applications such as implantation devices. Unfortunately, the high composition of nickel in this alloy can be harmful to human body, if its exposure exceeds a threshold value. Therefore, an innovative electrical discharge coating technique was investigated and proposed in this study to develop minimal microdefects formation with high corrosion resistance through fractional factorial design of experiment. The results showed that discharge duration mostly dominated the material deposition, microcracks, and porosity fraction up to 72%, due to the impact of the intensity of discharge energy. There was also a pronounced effect of titanium powder concentration in the deionized water on the percentage of titanium and nickel elements, and microcracks formation. The powder suspension enhanced the recast layer formation through the increment of layer density, which covered up the Ni-rich region and diminished the microcrack formation. An optimized substrate recorded the lowest corrosion current, I_{corr} and highest corrosion voltage, E_{corr} at 3.43 x 10^{-6} µA/cm² and -0.07 V respectively, thus exhibited an outstanding corrosion resistance rate at only 8.57 µm/year in phosphate-buffered saline solution, due to the low nickel concentration, low microcracks and low porosity fraction in the recast layer. Therefore, the results obtained within this study presented an initial step towards assessing the feasibility of applying the electro-discharge process to biomaterials, including nickel-titanium shape memory alloy. Further exploration, involving both *in-vitro* and/or *in-vivo* studies, is essential to thoroughly evaluate the performance of the coating obtained from the process.

Keywords: NiTi SMA; Electrical discharge coating; Microcrack; Porosity; Corrosion resistance.

1. Introduction

Nickel-titanium shape memory alloy (NiTi SMA), simply called Nitinol, is a new class of smart materials that is widely used to develop medical and surgical devices, such as coronary stents, scoliosis correction rods, bone fracture fixations devices, arc-wires and intramedullary nails, to mention but a few. NiTi SMA has superior properties of remarkable recovery shape after deformation with respect to the induction of two thermomechanical behaviours: shape memory effect and super-elasticity. These properties are mainly applied to conduct less invasive surgery on the patient with good fixation of the devices in the body after implantation. Besides, the alloy has excellent mechanical properties, such as high fatigue, strength, near-to-bone elastic modulus, less density and wear resistance [1]. However, the biocompatibility of the alloy is still questioned, due to the high nickel content that nearly equi-atomic to the titanium. During corrosion, the nickel leached from the alloy surface and induced severe local tissue irritation, necrosis and cancer [2]. The native passivation of oxide film that naturally formed on the alloy surface is incapable of withstanding the corrosive environment of body fluid for a long implantation period, due to the formation of very thin layer thickness of oxide film.

Decades ago, the biocompatibility issue of NiTi SMA has attracted interest to produce a biocompatible coating layer on the material. Many attempts have been reported to produce an appropriate coating layer with high corrosion resistance that substantially prevents the excessive migration of toxic elements into the body. Simultaneously, the modified surface should be adequate to promote cell adhesion and proliferation to expedite the biological self-healing process [3]. Among techniques that have been applied to alter the NiTi SMA surface include sol-gel technology [4], selective oxidation [5], anodization in an acid electrolyte [6], autoclave and boiling

water [7] and hydrothermal method [8]. These techniques are used to enhance the formation of a native oxide layer in a thin film thickness on the alloy surface. However, the film may not withstand a corrosive environment and longer loading conditions in the body, due to the poor adhesion and bond strength of the coating layer [9]. Other standard coating methods, such as thermal spraying, electroplating, physical vapor deposition (PVD) and chemical vapor deposition (CVD) have been observed to satisfy the formation of the coating with good surface performances. However, it requires particular and costly apparatus setup and process conditions. Moreover, the processes are also challenging to control in terms of the coating thickness and location area on the workpiece surface [10].

Moving forward, electrical discharge coating (EDC) is a revolutionary surface modification technique adapted from the electrical discharge machining (EDM) process. This process uses repetitive electrical pulses to generate heat energy on the workpiece surface within a temperature range of 8,000 to 12,000 °C [11], which can melt and evaporate metal alloys into debris, irrespective of their mechanical properties. At the end of the erosion, the debris are flushed away from the machined area by high flow rate of dielectric fluids. On the other hand, a large portion of the molten area re-solidifies and remains on the machined surface. These residues lead to the formation of a significantly hard recast layer, due to the quenching phenomena in the dielectric fluid. The layer comprises an inter-mixture of molten metals from the workpiece, tool electrode and dielectric decompositions. In EDC operation, the material erosions on the workpiece and electrode surfaces are the main indicator of the process performance. The erosion level depends on the intensity of the discharge generation. During the process, the discharge energy is significantly affected by the electrical parameter settings, such as discharge duration, peak current, voltage and duty cycle [12-16]. Among the parameters, the discharge duration was the most

significant parameter from the previous literature, due to its dominating effect on erosion performance. The recast layer was also significantly produced by increasing the discharge duration, as reported by Furutani et al. [17] as well as Hasc and Caydas [18]. Meanwhile, Chen et al. [19] observed that a longer discharge duration significantly increased the composition of the oxide layer phase on the pure titanium surface, when performing the EDC process in deionized (DI) water. However, the surface crack was propagated significantly on the coated surface with the increment of the discharge energy by the discharge duration [14].

Meanwhile, the surface characteristic of the recast layer coatings can be significantly improved through additive powder mixed with the dielectric fluid. Bhattacharya et al. [20] reported a significant deposition of additive powder on the workpiece surface that enhanced the surface finish, reduced the microcracks formation and increased the microhardness. The increment of electrical conductivity of the mixed dielectric fluid resulted to a smoother surface finish, due to even spark energy distribution on the workpiece. In principle, the recast layer formation is initiated by the formation of conductive bridging of the powder particles in the sparking gap, due to the capacitive effect. As shown in Fig. 1, the particle bridges are formed in the sparking gap when the open voltage is elevated. Then, the sparks are initiated, due to the chain breakage, and an explosion occurs. Lastly, the particles are re-bridged when a new pulse is initiated. During the sparking, a high temperature in a plasma channel melts the particles and then migrates into the melted pool on the workpiece surface.

Based on the aforementioned studies and in an attempt to further improve the properties and increase the application of NiTi SMA, further investigation into microdefects and corrosion resistance of NiTI SMA was proposed, using EDC process. Therefore, this present study aimed at

investigating into the use of EDC technique to develop the material with less formation of microdefect and high corrosion resistance.

2. Experimental procedures

2.1 Machine, material and preparation of samples

The experiment was performed using EA8 Mitsubishi die sinker machine. The material substrate used was nickel-titanium (NiTi) shape memory alloy (SMA) that was purchased from Baoji Hanz Metal Material Corp., Shaanxi, China. This material is classified as a medical-grade alloy suitable for medical devices and surgical implants, according to the ASTM F2063-12 standard. The substrate was prepared to the dimension size of 70 × 70 × 5 mm. Prior to the EDC process, the NiTi substrate and titanium electrode surfaces were prepared via several mechanical techniques, namely, grinding, polishing, and etching. These techniques are essential to produce a flat parallel surface between the substrate and electrode and remove unwanted material layers on both surfaces. During the grinding process, the surfaces were abraded using silicon carbide (SiC) papers of 180, 400, 800, 1000 and 2000 grit sizes to obtain a near-mirror finish. Then, the surfaces were polished, using monocrystalline diamond suspension and etched using Kroll's reagent formulation of 6.0 ml of HNO_3, 2.0 ml of HF and 92 ml of distilled water for 10 seconds before rinsed. Table 1 presents the chemical composition and mechanical properties of the substrate from the certificate test of the supplier. The transformation temperature was obtained from the differential scanning calorimetry (DSC) test. For the tool electrode, grade II of pure titanium rod of 99.99% purity was used with dimensional (diameter x length) size of 10 x 8 mm. The tool electrode was attached on another pure titanium rod of 10 x 50 mm by a copper adhesive film and fixed on a machine tool holder. The DI water was utilized as the dielectric fluid to encourage the formation of an oxide layer, as

the recast material. For selected trials in the experimental layout, the DI water with mixed titanium powder were used as the dielectric fluid. The mixing procedure were carried out by adding 1.2 gram of pure titanium powder with average diameter of 0.77 nm in 200 litre of DI water and sonicated, using an ultrasonic device at amplitude of 10% for 10 minutes. This procedure was conducted to increase the dispersion of the titanium particles in the DI water and avoid significant particulate settlement on the bottom during the EDC trials.

2.2 Experimental approach

The experimental works were planned based on a statistical method to evaluate the process performance and surface coating quality, thus, optimization was not part of the procedures carried out in this present work. The experimental layout was constructed in a half fractional factorial design of 2^{6-1} in resolution VI. This design has an appropriate alias structure that permitted all the essential estimation on the main effects and interactions with reasonable number of trials and more cost effective, when compared with the full factorial design [21, 22]. In addition, the vital estimates are not completely present in saturated designs like the Taguchi's method, which calls for more trials to gather the information. Table 2 presents the six parametric conditions in the experimental design. The analysis of variance (ANOVA) technique was employed to evaluate the parameters on the material deposition and microdefects. The P-value below 0.05 was selected to justify the significant levels of the main effects and parameter interactions.

2.3 Experimental setup and measurement

Fig. 2 depicts the schematic of the experimental setup. Voltage and current probes were attached on a tool holder and reservoir to monitor the current and voltage signals during the process, using

a high bandwidth digital oscilloscope. The trials were performed in 90 minutes with new location for each experimental condition on the substrate surface. The energy dispersive x-ray (EDX) analysis was implemented to examine the elemental percentage of titanium and nickel on the treated surface. The measurement was performed, using the Bruker-Quantax 70 EDS system integrated with Hitachi TM3000 scanning electron microscopy (SEM). Three location points on the treated surface were measured for each elemental percentage. An average percentage was calculated and used for the ANOVA analysis.

Then, the microcracks and porosity fraction were measured on the topography images that were captured by the SEM (brand: JEOL and model: JSM-6010LV) under 1000× magnification. The measurement was conducted using an open-source image processing software, namely ImageJ on three location points of the substrate surface. Meanwhile, the corrosion test was carried out using an electrochemical technique via potentiodynamic polarization, according to ASTM F2129 standard. The test was conducted in phosphate-buffered saline (PBS) solution at approximately 37 °C and pH 7.4 to mimic the body environment. By using Autolab (model: PGSTAT302N), a constant scan rate of 1.0 mV/s from -0.8 to 1.0 V with respect to open circuit potential (OCP) was used to evaluate the electrochemical reaction on a standard three-electrode system. The electrode system included the saturated calomel electrode (SCE) as a reference electrode, platinum plate as the counter electrode and NiTi substrate, as the working electrode. The untreated side of the substrates were covered with epoxy resin paint in order to localize the reaction in the target area. The OCP was maintained for 1 hour in the PBS solution to attain a constant state. At the end, the captured data was analysed, using NOVA software. For this corrosion test, several substrates were selected based on the result of the statistical analyses. The selected substrates were those with the thinnest recast layer thickness (RLT), those with a high formation of RLT (under both pure and

mixed DI water), the finished substrate (which is a high RLT substrate formed after a finishing operation), and the optimized substrate (which is a substrate with the lowest percentage of nickel, microcracks, and porosity fraction).

3. Results and discussion

3.1 Material deposition on the NiTi alloy

The EDC process possesses the ability to generate a recast layer on the surface of the substrate. The recast layer formation is largely influenced by the process parameters, especially from the discharge duration setting, as depicted in Fig. 3. The composition of this formed layer on the substrate surface is largely determined by factors such as the material of the electrode, the material of the sample, the dielectric fluid, and the suspension of material in the dielectric. This section presented a statistical analysis of how EDC parameters influence the deposition of titanium and the inhibition of nickel on the substrate surface. The results of analysis of variance as shown in Fig. 4 indicates that powder mixed in DI water increased the titanium deposition significantly on the substrate. In the model effect, this parameter contributed up to 53% of the response performance. With the mixture of additive powder in the DI water, the extreme temperature of the plasma channels melted nearby additive particles and entrapped them in conductor bridges. These particles migrated to the substrate surface, due to high negative pressure and bubbles collapse. This result can be established by observing the current waveform of the discharges, as depicted in Fig. 5. The effect of conductor bridges on the waveform can be observed significantly by the multi sub-discharges formation on the electrical signal under 6 g/l of powder concentration. Nonetheless, the additive powder in DI water also helped to intensify titanium particle suspension, thus significantly reduced the nickel element on the substrate. In another context, the EDC process also

produced debris particles suspended in the dielectric fluid that can cause abnormal discharge pulses [23]. The excessive mixed additive powder could affect the process stability and performance. The small size of the nano powder particles could not increase the discharge gap expansion, which led to process stability [24]. But the increment of the powder concentration can interrupt the effectiveness of the discharge generation, especially under low operating conditions.

The second key factor of the main effect was the B-discharge duration. A long discharge time increased the titanium percentage on the substrate surface. This can be attributed to the significant erosion of the tool electrode, due to the high discharge duration. The high tool electrode erosion increased the possibility of the titanium debris particles to be migrated on the substrate surface and diffused into the melted pool. The high intensity of the discharge energy also produced a Ti-rich oxide matrix (titanium sesquioxide, Ti_2O_3) on the substrate surface, reflecting the high percentage of titanium on the recast layer, see Fig. 6(b). Meanwhile, the nickel compound in the recast layer can be diminished by the high composition of the Ti-rich oxide phase as shown in Fig. 6c. A higher migration of titanium particles assisted the Ti-rich phase composition, due to tool erosion.

3.2 Microdefects formation

Fig. 7 depicts the half-normal probability that shows the significant terms to the microcracks formation and porosity fraction on the NiTi substrate. It was apparent that there were seven significant parameters and interaction factors of microcracks model that deviated from the normal distribution line. For porosity fraction, only B-discharge duration, interaction of gap voltage and powder concentration (interaction EF) were significant to the model. The discharge duration dominated the effect on the microcracks formation and porosity fraction, which contributed up to 18 and 72%, respectively. By increasing the discharge duration, significant microcracks was

formed on the recast surface, as shown in Fig. 8(a). A long discharge duration promoted extreme thermal stresses on the recast material. The thermal stresses increased significantly, because the high parameter setting produced a great volume of melted material. The melted material rapidly cooled than the parent material, leading to an increase in the internal stress of the recast layer and subsequently the microcracks formation. This result was consistent with the reports from Chen et al. [17], Algodi et al. [26] and Salmaliyan et al. [14] that claimed a significant effect of discharge duration on the microcracks formation, due to the high spark energy and thermal contraction on the modified layer. Meanwhile, the increase in discharge duration also significantly increased the porosity formation on the surface. Due to the long discharge duration, a higher electron emission was produced that encouraged the decomposition of DI water into a higher volume of gases released, such as oxygen and hydrogen. At the end of the pulse, the gases tended to dissolve in the molten material through the turbulent movement of the fluid caused by the plasma channel collapse [26]. The absorbed gases were released from the molten material, due to the rapid quenching that subsequently produced open porosities on the recast surface [23]. The result was in agreement with that of Tyagi et al. [24], who reported higher formation of pores, fused zone and voids, due to the arcing condition at 90% of duty with an increase in the discharge duration.

Furthermore, the Ti powder mixed in the DI water significantly reduced the microcracks density on the NiTi substrate, as depicted in Fig. 8(b). The parameter improved the surface quality up to 16% contribution. During the EDC process, the Ti powder was melted by the discharge generation and subsequently migrated onto the substrate surface. The migration of the additive powder increased the volume of melted material on the substrate and reacted to improve the material shortage, which can be attributed to the shrinkage during re-solidification of the melted material. These results were similarly reported by Wu et al. [25], Xie et al. [26] and Prakash et al.

[16] that discovered the suppression on the thermal stress impact that reduce the microcracks density when using additive powder mixed in dielectric fluid. The discharge energy was dispersed randomly throughout the substrate surface, due to the formation of multiple sub-discharges. In this current case, the effectiveness of the sub-discharges can only be achieved by utilizing the micro dimension size of powder particles. As shown in Fig. 9, the microcracks were severely propagated on the treated surface under high discharge duration, when compared with the low operating condition. The severity of the microcracks was evidenced in term of the width, length and number of cracks on the surface. For the substrate prepared under high powder concentration, the surface was relatively dense and no appreciable microcracks were formed.

Fig. 10 shows the effect of the discharge duration on the porosity fraction of the NiTi substrate. The increase in discharge duration significantly increased the porosity formation on the surface. Due to the long discharge duration, a higher electron emission was produced that encouraged the decomposition of DI water into a higher volume of gases released, including oxygen and hydrogen. Meanwhile, since the high discharge duration increased the volume of the molten material on the substrate, hence more gases were dissolved in the molten. This circumstance also occurred under the high adhesion of additive material on the surface, due to the increased titanium powder concentrations.

More also, Fig. 11 depicts the surface condition under the different powder concentrations with a high discharge duration setting. Although, the F-powder concentration had no significant effect on the porosity formation, but it can be well observed that many foamy like-shaped porous were produced in the recast layer. It occurred because of the increase in the molten material volume, hence tended to dissolve high solubility gases. The gases accumulated in large cavities and suppressed the formation of small gas bubbles on the surface. Therefore, less small voids

formation was observed on the substrate, which operated with 6 g/l of powder concentration mixed in DI water. As a result, the surface area was smoothly formed even though porosities were almost entirely observed in the scaffold structures. Meanwhile, Fig. 12 shows the effect of the significant interaction between the gap voltage and powder concentration on the porosity fraction. Under a normal condition, the gap voltage influences the gap distance between the electrode and the substrate surface. This condition can slightly reduce the impact of the discharge duration. Therefore, the porosity formation on the substrate can be alleviated, because of the low dissolved gases bubbles in the molten material. However, with the mixed additive powder, a longer gap distance encouraged a higher accumulation of powder particles in the gap. With sufficient discharge intensity, higher adhesion of the titanium particles was evidenced, which elevated the porosity formation on the substrate surface. Fig. 13 depicts the surface condition of the substrate under high gap voltage with different concentrations of titanium powder. The surface was more deteriorated by a few deep porous formations under the high powder concentration (Fig. 13(b)). However, a smooth surface with fewer material globules was still visible on the substrate.

3.3 Corrosion resistance

Fig. 14 shows the potentiodynamic polarization curves of the parent NiTi and several treated substrates. The curves depict no sign of pitting corrosion on all substrates. Through the Tafel extrapolation lines, a higher positive corrosion potential, E_{corr} of the curves indicated the difficulty level of the corrosion, which presented a good corrosion resistance of the substrate. It was evident that the parent material (NiTi SMA) recorded the lowest E_{corr} value, when compared with the treated substrates. It was further established that the treated substrates by the EDC operation produced better corrosion resistance than the uncoated material. The second curve with lower E_{corr}

was the substrate with high RLT. The E_{corr} was recorded at -0.50 V, which was marginally close to the E_{corr} value at -0.60 V recorded by the parent material, Table 3. Meanwhile, by adding 6 g/l of powder concentration in the DI water, the E_{corr} significantly reduced up to 18% on the high RLT substrate when compared with the substrate that was operated in pure DI water. Moreover, a stepwise finishing operation on the high RLT substrate (under 6 g/l of powder concentration) further increased the E_{corr}. It had capability of increasing the E_{corr} of the substrate up to 7% from -0.41 to -0.38 V. Besides, a low RLT substrate under the low operating settings recorded a greater E_{corr} value, when compared with others. However, the best E_{corr} value was recorded with the optimized substrate at -0.07 V.

Beside the E_{corr} indicator, the corrosion current, I_{corr} was also a crucial parameter that influenced the corrosion property of the substrate. According to Zhang et al. [2], a small I_{corr} value indicated a low self-etching current in the corrosion kinetics, which implied a better corrosion resistance. The uncoated parent NiTi alloy material recorded the largest I_{corr} value of 253.77 $\mu A/cm^2$, when compared with the treated substrates as presented in Table 3. The lowest I_{corr} was recorded at 3.43×10^{-6} $\mu A/cm^2$ from the optimized substrate. It implied that the current flow was significantly inhibited by the coating layer of the optimized surface. In between the lowest and highest I_{corr} values, the finished substrate and the high RLT substrate of 6 g/l of powder concentration exhibited the corrosion current value of 19.97 and 52.42 $\mu A/cm^2$, respectively. Although, the low RLT substrate had a good E_{corr} value, the I_{corr} was higher than the finished and high RLT substrates. Therefore, since the corrosion rate (CR) was mainly depended on the I_{corr} value, as stated by the CR formula in ASTM G59-97 standard, the low RLT substrate was estimated to have higher yearly CR when compared with the aforementioned treated substrates. Table 3 also presents the polarization resistance (R_p) of the substrates. The parent material had the

lowest R_p value, which was nearly 37% less than the high RLT substrate of 6 g/l powder concentration and the finished substrate. Meanwhile, the optimized substrate recorded the highest R_p at 17.9 MΩ, which was approximately 6200 times greater than the parent material. Therefore, the optimized substrate was evidently observed to have marginally capability of inhibiting the corrosion rate of 8.57 μm/year.

4. Conclusions

The experimental study has been performed to evaluate the effects of EDC parameters on the material deposition, microcracks and corrosion resistance of NiTi shape memory alloy. Based on the results obtained, the following concluding remarks can be deduced.

- Discharge duration mainly affected all the performance measures of titanium percentage, it contributed up to 53%. With nickel percentage, microcracks and porosity formation contributed up to 18 and 72% respectively, due to the influence of the discharge energy intensity. It could significantly enhance the titanium percentage but produced poor surface quality through increment of microcracks and porosity formation. This can be attributed to a long discharge duration, which generated high thermal stress in a large volume of molten material and then induced the microdefects formation significantly during the re-solidification period.
- Powder concentration in the DI water played an important role in the EDC process, particularly to increase titanium percentage and alleviate the nickel on the recast layer. It also significantly contributed up to 16% of reduction in the microcracks formation that occurred, due to the internal stress during the re-solidification of the molten material. However, this

parameter was unable to reduce the porosity fraction on the substrate but led to an increase in the development of foamy-shape porosity on the surface.

- Among the tested substrates, the optimized substrate recorded an outstanding corrosion rate of 8.57 µm/year, due to the lowest I_{corr} and highest E_{corr} at 3.43 x 10^{-6} µA/cm² and -0.07 V, respectively. This can be attributed to the low nickel percentage in the recast layer formation, microcracks and porosity fraction on the surface, which significantly enhanced the corrosion resistance of the NiTi SMA. Hence, the coating thickness may not be the main indicator for good corrosion resistance of the substrates.
- Overall, the afore-stated results mark the first phase in determining the feasibility of employing EDC process on nickel-titanium shape memory alloy. Further investigation is necessary to explore the performance of the coating produced by the process, such as examining the toxicity level and proliferation of the living tissues through *in-vitro* and/or *in-vivo* studies.

Statements & Declaration

a. Funding:

The authors gratefully acknowledge the financial support from Fundamental Research Grant Scheme FRGS/1/2017/TK03/UNIMAP/03/5 under UniMAP Project Code: 9003-00633, which was granted by Ministry of Higher Education, Malaysia.

b. Conflicts of interest/Competing interests (include appropriate disclosures)

The authors declare that they have no known competing financial interests or personal relationships that could have appeared to influence the work reported in this paper.

c. Availability of data and material (data transparency), and code availability (software application or custom code).

Not applicable

d. Ethics approval (include appropriate approvals or waivers)

Not applicable

e. Consent to participate (include appropriate statements)

Not applicable

f. Consent for publication (include appropriate statements)

The authors provide consent for the publisher to publish the manuscript

g. Authors' contributions (optional: please review the submission guidelines from the journal whether statements are mandatory)

All authors have read and agreed to the published version of the manuscript. Conceptualization, methodology, writing, review and editing for this research were performed by all of the authors. Data curation, analysis and validation were conducted by Ahmad Fairuz Mansor, and research supervision was performed by Azwan Iskandar Azmi.

References

[1] A. F. Mansor, R. Jamaluddin, A. I. Azmi, T. C. Lih, and M. Z. M. Zain, "Surface modification of nitinol by using electrical discharge coatings in deionized water," *IOP Conf Ser Mater Sci Eng*, vol. 670, no. 1, 2019, doi: 10.1088/1757-899X/670/1/012010.

[2] L. Zhang *et al.*, "Graphene enhanced anti-corrosion and biocompatibility of NiTi alloy," *NanoImpact*, vol. 7, pp. 7–14, 2017, doi: 10.1016/j.impact.2016.10.003.

[3] C. Prakash, H. K. Kansal, B. S. Pabla, S. Puri, and A. Aggarwal, "Electric discharge machining - A potential choice for surface modification of metallic implants for orthopedic applications: A review," *Proc Inst Mech Eng B J Eng Manuf*, vol. 230, no. 2, pp. 331–353, 2016, doi: 10.1177/0954405415579113.

[4] D. P. Aun *et al.*, "Development of a flexible nanocomposite TiO2 film as a protective coating for bioapplications of superelastic NiTi alloys," *Appl Surf Sci*, vol. 375, pp. 42–49, 2016, doi: 10.1016/j.apsusc.2016.03.064.

[5] M. Pohl, T. Glogowski, C. Hessing, and F. Unterumsberger, "Formation of titanium oxide coatings on NiTi shape memory alloys by selective oxidation," *Materials Science and Engineering A*, vol. 482, pp. 123–126, 2008, doi: 10.1016/j.msea.2007.02.151.

[6] N. Ohtsu and Y. Hirano, "Growth of oxide layers on NiTi alloy surfaces through anodization in nitric acid electrolyte," *Surf Coat Technol*, vol. 325, pp. 75–80, 2017, doi: 10.1016/j.surfcoat.2017.06.021.

[7] A. Michiardi, C. Aparicio, J. A. Planell, and F. J. Gil, "New oxidation treatment of NiTi shape memory alloys to obtain Ni-free surfaces and to improve biocompatibility," *J Biomed Mater Res B Appl Biomater*, vol. 77, no. 2, pp. 249–256, 2006, doi: 10.1002/jbm.b.30441.

[8] F. T. Cheng, P. Shi, and H. C. Man, “A preliminary study of TiO2 deposition on NiTi by a hydrothermal method,” *Surf Coat Technol*, vol. 187, no. 1, pp. 26–32, 2004, doi: 10.1016/j.surfcoat.2004.01.023.

[9] C. Prakash, H. K. Kansal, B. S. Pabla, S. Puri, and A. Aggarwal, “Electric discharge machining - A potential choice for surface modification of metallic implants for orthopedic applications: A review,” *Proc Inst Mech Eng B J Eng Manuf*, vol. 230, no. 2, pp. 331–353, 2016, doi: 10.1177/0954405415579113.

[10] P. J. Liew, C. Y. Yap, J. Wang, T. Zhou, and J. Yan, “Surface Modification and Functionalization by Electrical Discharge Coating - ALiew, P. J., Yap, C. Y., Wang, J., Zhou, T., & Yan, J. (2020). Surface Modification and Functionalization by Electrical Discharge Coating - A Comprehensive Review. International,” *International Journal of Extreme Manufacturing*, vol. 2, pp. 1–32, 2020, doi: 10.1088/2631-7990/ab7332.

[11] S. Abdulkareem, A. Ali Khan, and M. Konneh, “Cooling effect on electrode and process parameters in EDM,” *Materials and Manufacturing Processes*, vol. 25, no. 6, pp. 462–466, 2010, doi: 10.1080/15394450902996619.

[12] A. Ghafarinazari, “Electrical discharge machining characteristics of nickel−titanium shape memory alloy based on full factorial design,” *J Intell Mater Syst Struct*, no. May 2014, 2013, doi: 10.1177/1045389X13476147.

[13] V. Babu, J. S. Soni, and M. L. Rao, “Analysis and evaluation of heat affected zones (HAZ) of the work piece surface machined using different electrode by Die-sinking EDM of EN-31 die steel",International Journal Of Engineering And Science (IJES),” *Int J Eng Sci (Ghaziabad)*, vol. 5, no. 3, pp. 37–42, 2016.

[14] M. Salmaliyan, F. Malek Ghaeni, and M. Ebrahimnia, "Effect of electro spark deposition process parameters on WC-Co coating on H13 steel," *Surf Coat Technol*, vol. 321, pp. 81–89, 2017, doi: 10.1016/j.surfcoat.2017.04.040.

[15] M. M. Bahgat, A. Y. Shash, M. Abd-Rabou, and I. S. El-Mahallawi, "Influence of process parameters in electrical discharge machining on H13 die steel," *Heliyon*, vol. 5, no. 6, p. e01813, 2019, doi: 10.1016/j.heliyon.2019.e01813.

[16] C. Prakash, H. K. Kansal, B. S. Pabla, and S. Puri, "Experimental investigations in powder mixed electric discharge machining of Ti–35Nb–7Ta–5Zrβ-titanium alloy," *Materials and Manufacturing Processes*, vol. 32, no. 3, pp. 274–285, 2017, doi: 10.1080/10426914.2016.1198018.

[17] K. Furutani, H. Sato, and M. Suzuki, "Influence of electrical conditions on performance of electrical discharge machining with powder suspended in working oil for titanium carbide deposition process," *International Journal of Advanced Manufacturing Technology*, vol. 40, pp. 1093–1101, 2009, doi: 10.1007/s00170-008-1420-x.

[18] A. Hasc and U. Caydas, "Electrical discharge machining of titanium alloy (Ti – 6Al – 4V)," *Appl Surf Sci*, vol. 253, pp. 9007–9016, 2007, doi: 10.1016/j.apsusc.2007.05.031.

[19] S. L. Chen, M. H. Lin, G. X. Huang, and C. C. Wang, "Research of the recast layer on implant surface modified by micro-current electrical discharge machining using deionized water mixed with titanium powder as dielectric solvent," *Appl Surf Sci*, vol. 311, pp. 47–53, Aug. 2014, doi: 10.1016/j.apsusc.2014.04.204.

[20] A. Bhattacharya, A. Batish, and N. Kumar, "Surface characterization and material migration during surface modification of die steels with silicon , graphite and tungsten powder in EDM process Surface characterization and material migration during surface modification of die

steels with silicon , g," *Journal of Mechanical Science and Technology*, vol. 27, no. 1, pp. 133–140, 2013, doi: 10.1007/s12206-012-0883-8.

[21] A. Mazen, B. McClanahan, and J. M. Weaver, "Factors affecting ultimate tensile strength and impact toughness of 3D printed parts using fractional factorial design," *International Journal of Advanced Manufacturing Technology*, vol. 119, no. 3–4, pp. 2639–2651, Mar. 2022, doi: 10.1007/s00170-021-08433-0.

[22] S. Beigmoradi and M. Vahdati, "Multi-objective optimization of a hatchback rear end utilizing fractional factorial design algorithm," *Eng Comput*, vol. 37, no. 1, pp. 139–153, Jan. 2021, doi: 10.1007/s00366-019-00813-1.

[23] S. Fattahi and H. Baseri, "Analysis of dry electrical discharge machining in different dielectric mediums," *Proceedings of the Institution of Mechanical Engineers, Part E: Journal of Process Mechanical Engineering*, vol. 231, no. 3, pp. 497–512, 2017, doi: 10.1177/0954408915611540.

[24] Y. Tzeng and C. Lee, "Effects of Powder Characteristics on Electrodischarge Machining Efficiency," *International Journal for Advanced Manufacturing Technology*, vol. 17, pp. 586–592, 2001.

[25] S.-L. Chen, M.-H. Lin, G.-X. Huang, and C.-C. Wang, "Research of the recast layer on implant surface modified by micro-current electrical discharge machining using deionized water mixed with titanium powder as dielectric solvent," *Appl Surf Sci*, vol. 311, pp. 47–53, Aug. 2014, doi: 10.1016/J.APSUSC.2014.04.204.

[26] S. J. Algodi, J. W. Murray, M. W. Fay, A. T. Clare, M. Miet, and P. D. Brown, "Electrical discharge coating of nanostructured TiC-Fe cermets on 304 stainless steel," *Surf Coat Technol*, vol. 307, pp. 639–649, 2016.

[27] C. Prakash, H. K. Kansal, B. S. Pabla, and S. Puri, "Processing and Characterization of Novel Biomimetic Nanoporous Bioceramic Surface on β-Ti Implant by Powder Mixed Electric Discharge Machining," *J Mater Eng Perform*, vol. 24, no. 9, pp. 3622–3633, 2015, doi: 10.1007/s11665-015-1619-6.

[28] R. Tyagi, A. K. Das, and A. Mandal, "Electrical discharge coating using WS2 and Cu powder mixture for solid lubrication and enhanced tribological performance," *Tribol Int*, vol. 120, no. December 2017, pp. 80–92, 2018, doi: 10.1016/j.triboint.2017.12.023.

[29] K. L. Wu, B. H. Yan, F. Y. Huang, and S. C. Chen, "Improvement of surface finish on SKD steel using electro-discharge machining with aluminum and surfactant added dielectric," *Int J Mach Tools Manuf*, vol. 45, pp. 1195–1201, 2005, doi: 10.1016/j.ijmachtools.2004.12.005.

[30] Z. J. Xie, Y. J. Mai, W. Q. Lian, S. L. He, and X. H. Jie, "Titanium carbide coating with enhanced tribological properties obtained by EDC using partially sintered titanium electrodes and graphite powder mixed dielectric," *Surf Coat Technol*, vol. 300, pp. 50–57, 2016, doi: 10.1016/j.surfcoat.2016.04.080.

Graphical Abstract

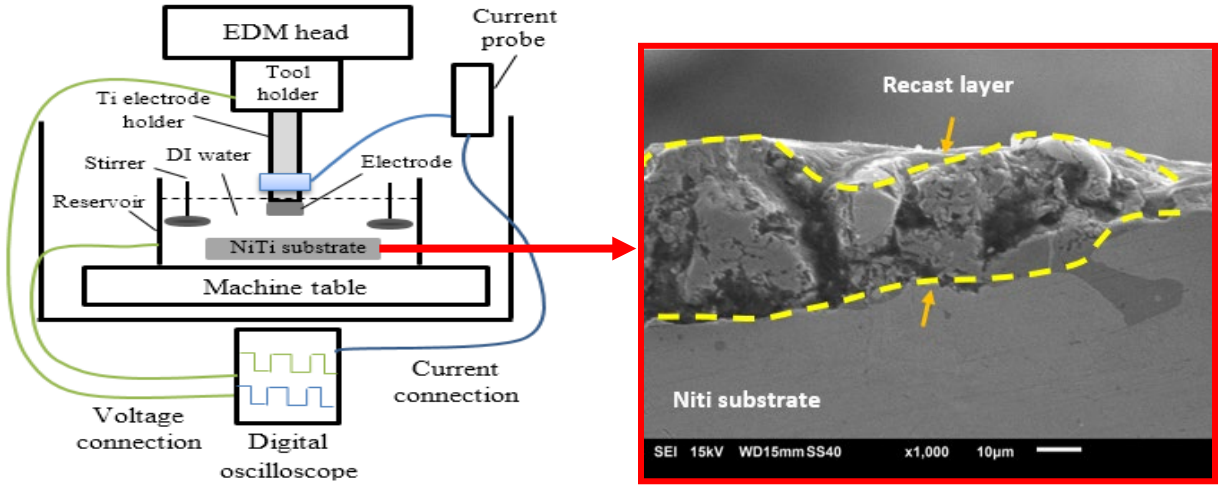

Figures

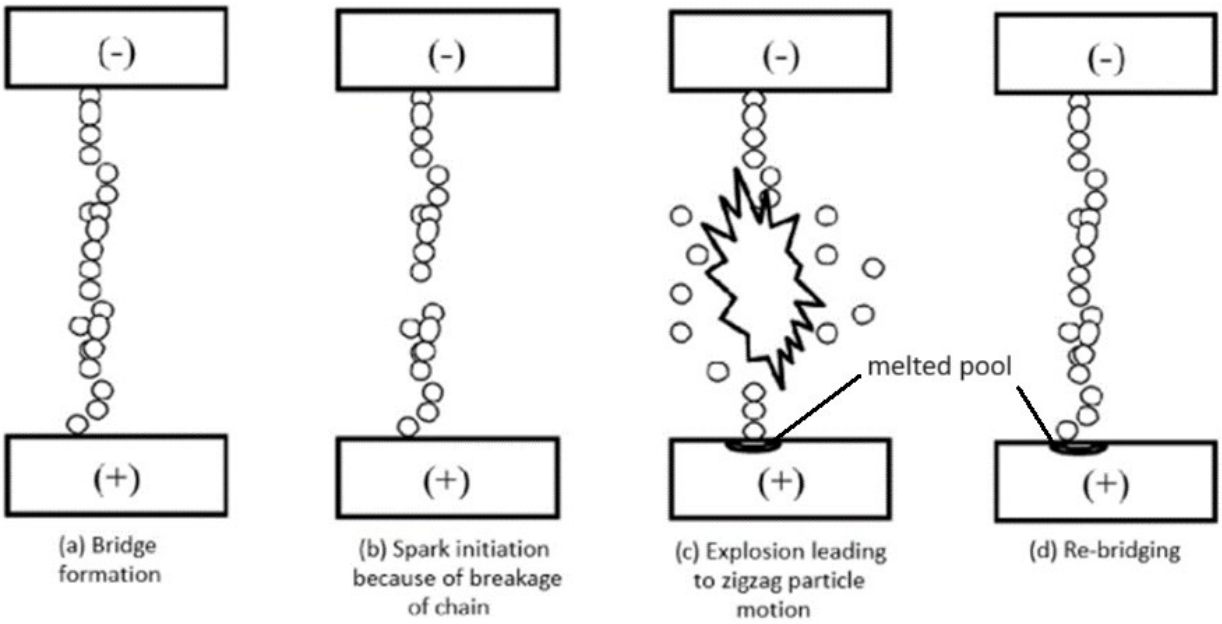

Fig. 1 Mechanism of the conductive bridges of powder particles [19]

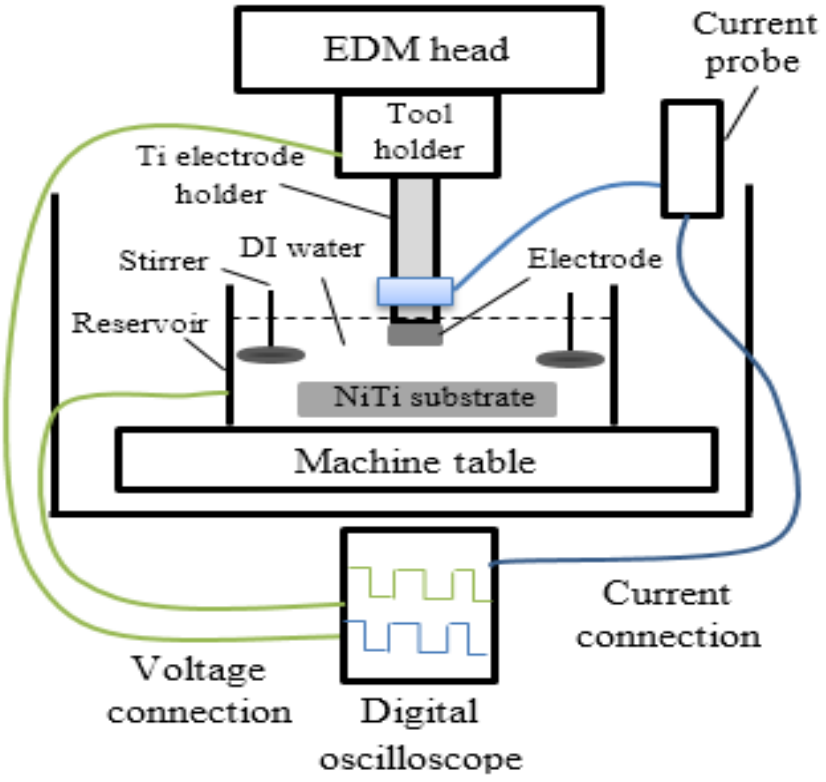

Fig. 2 Schematic diagram of experimental setup

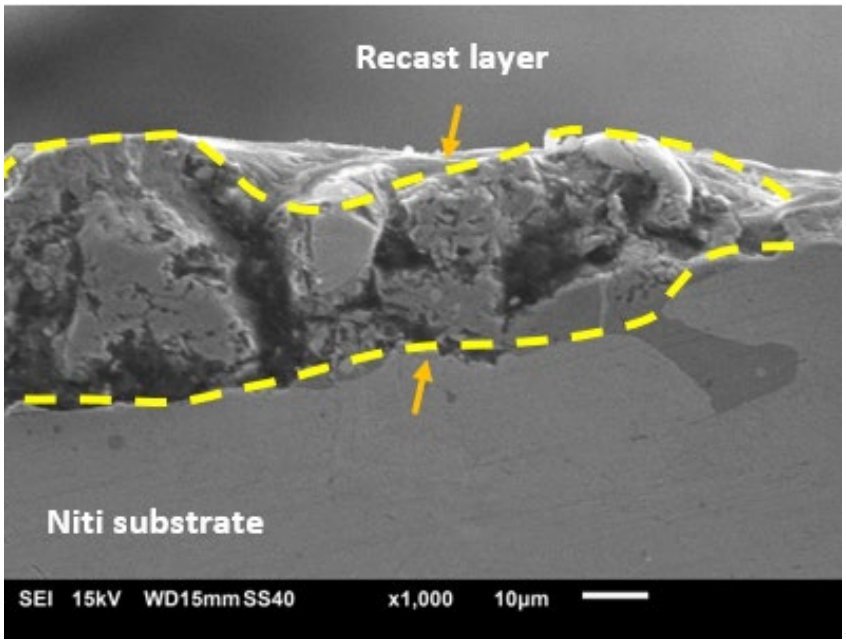

Fig. 3 SEM image of cross-sectioned substrate under high discharge duration

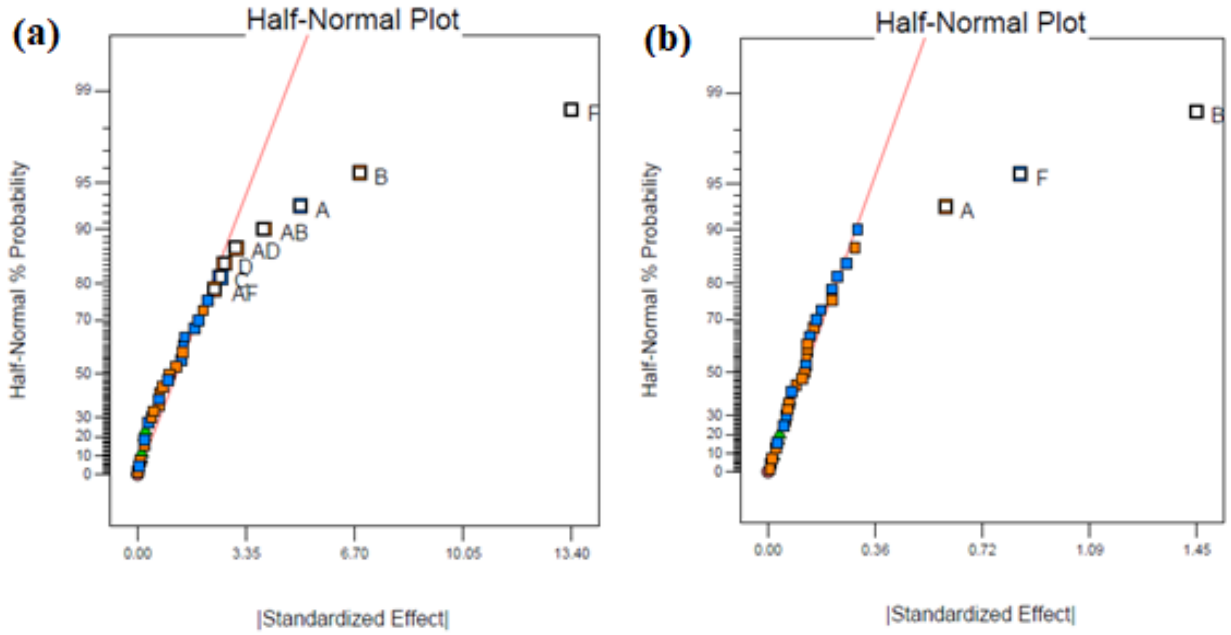

Fig. 4 Half-normal probability plot of (a) titanium and (b) nickel percentages

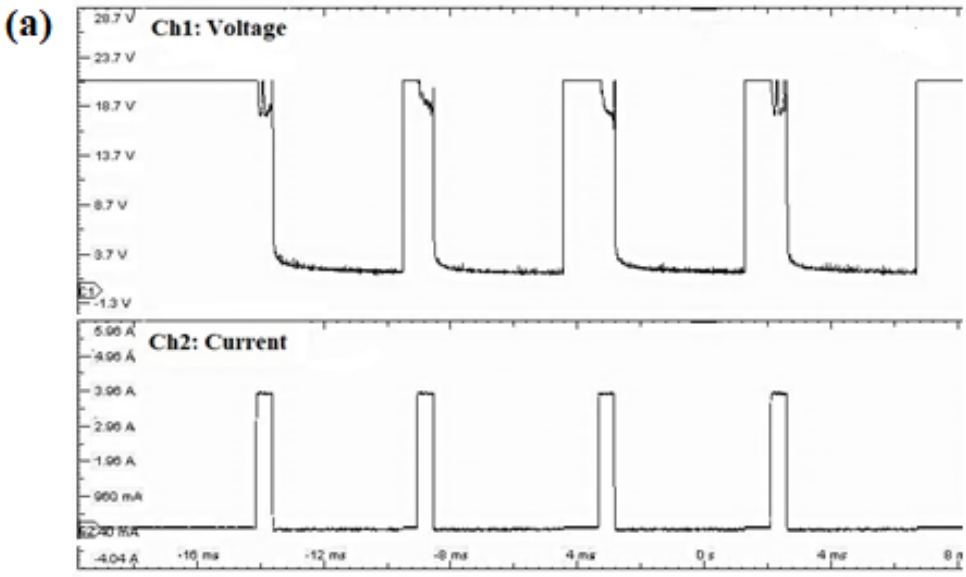

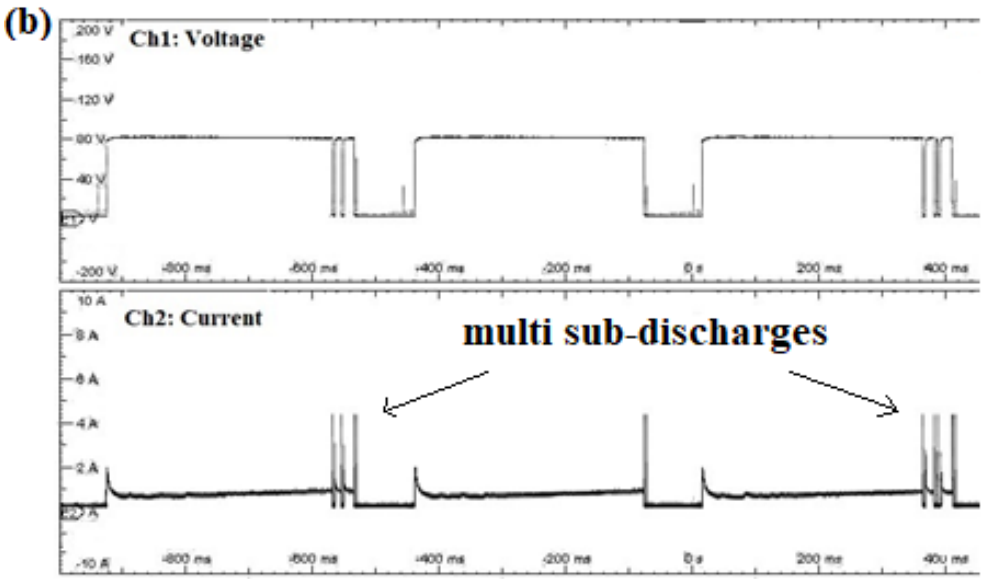

Fig. 5 Electrical waveforms under high discharge duration with (a) 0 and (b) 6 g/l of powder concentrations

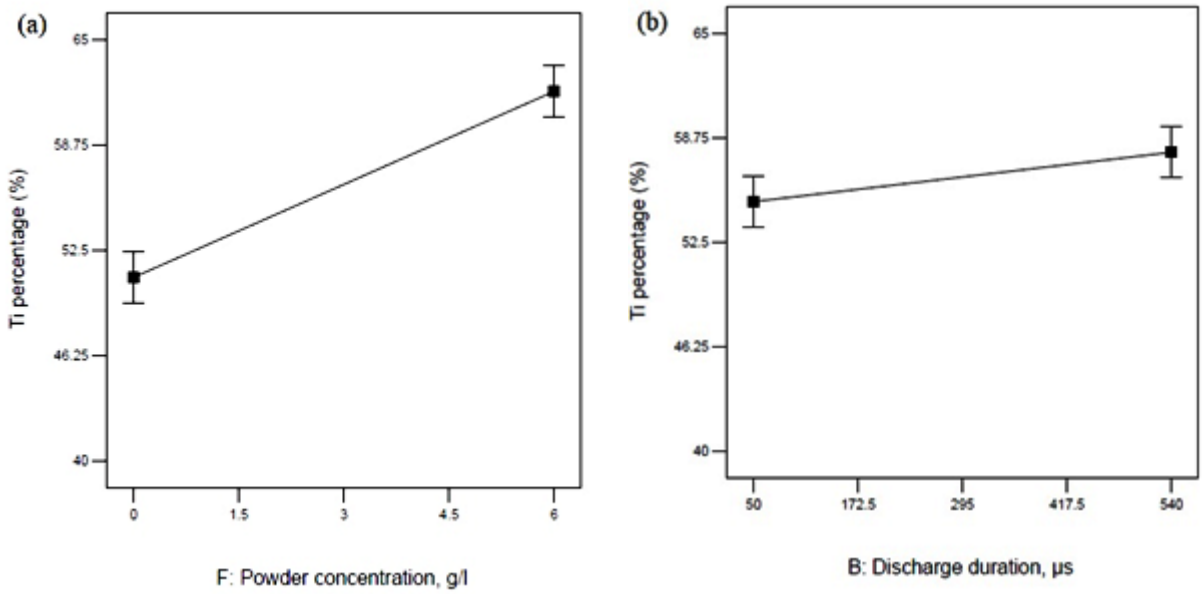

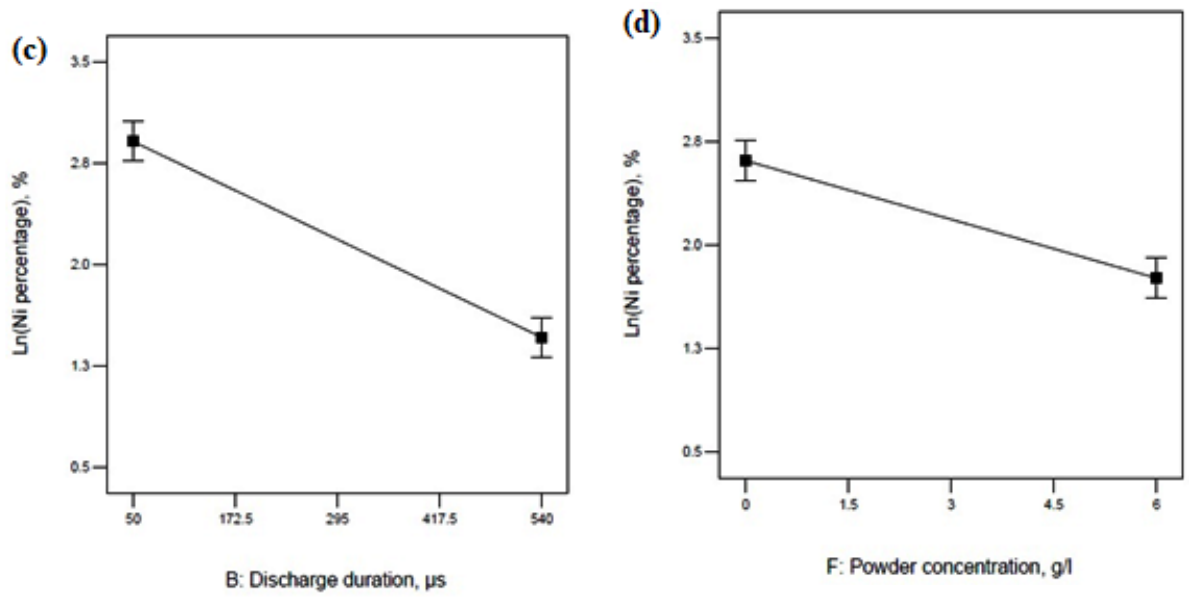

Fig. 6 Effects of absolute significant parameters on the deposition of titanium percentage, showing (a) F-powder concentration and (b) B-discharge duration as well as nickel percentage for (c) B-discharge duration and (d) F-powder concentration

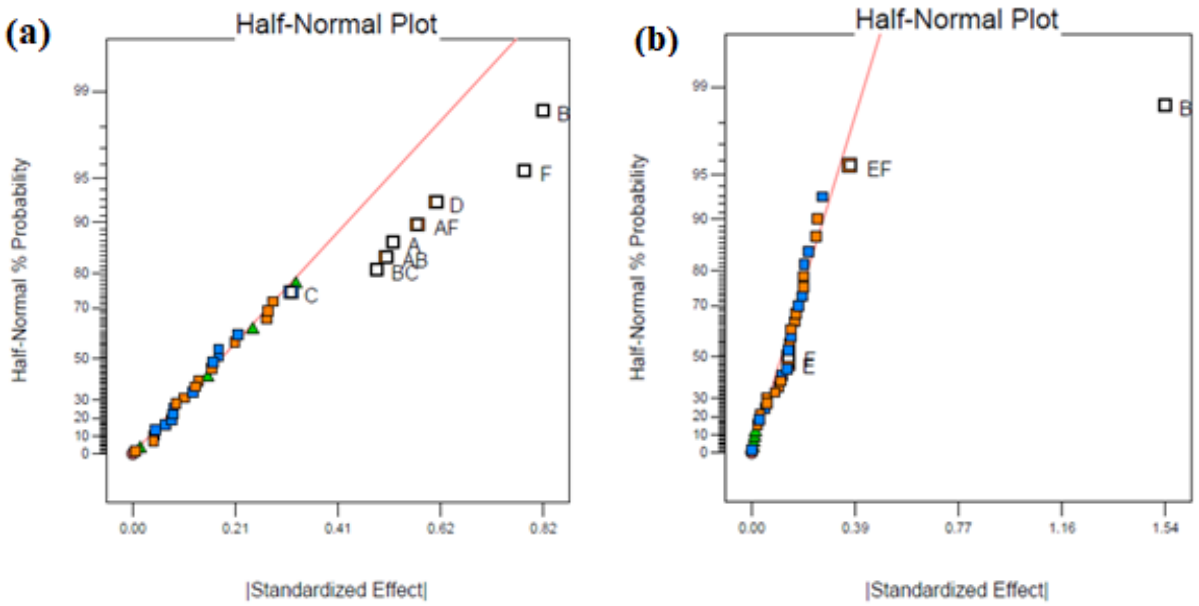

Fig. 7 Half-normal probability plot of (a) micro-cracks and (b) porosity fraction

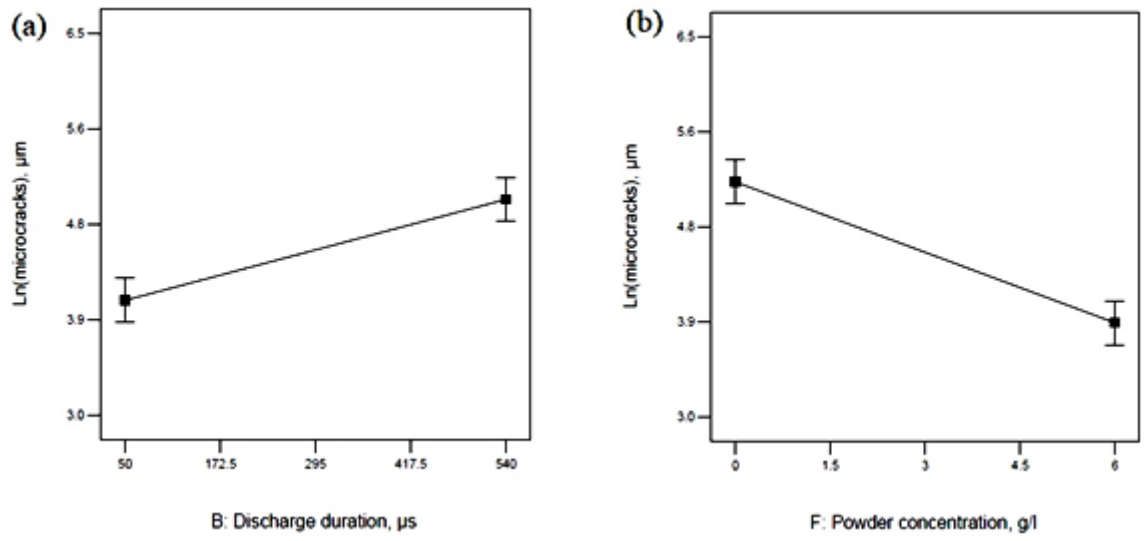

Fig. 8 Effects of absolute significant parameters on micro-cracks for (a) B-Discharge duration and (b) F-Powder concentration

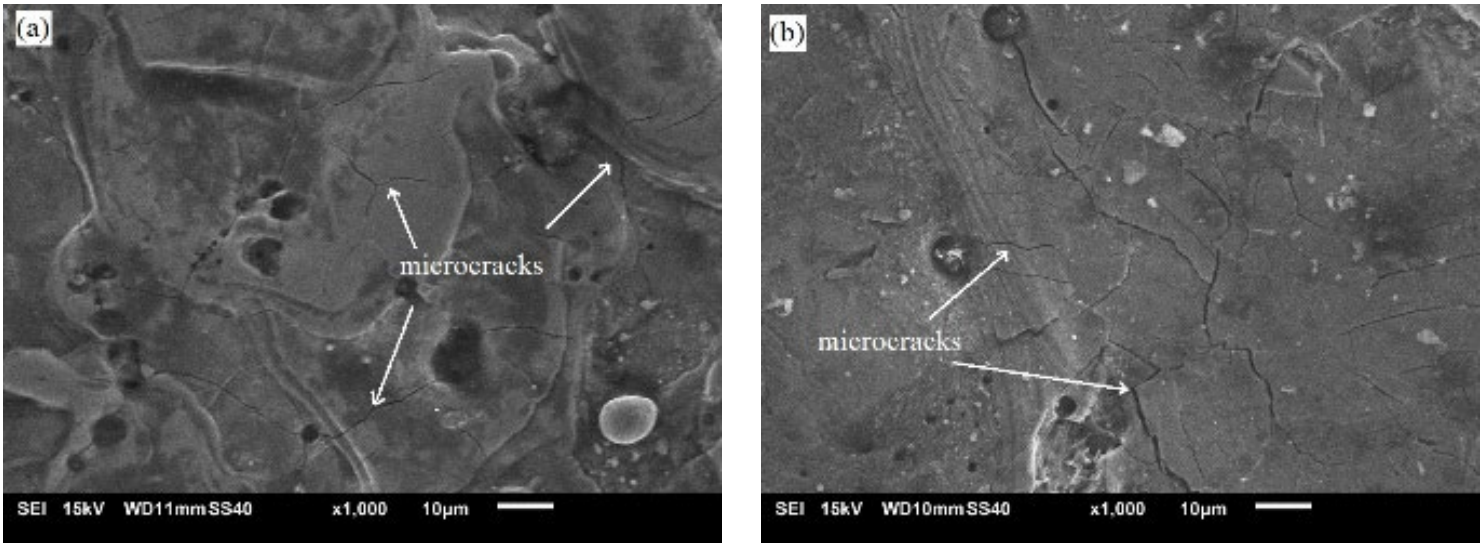

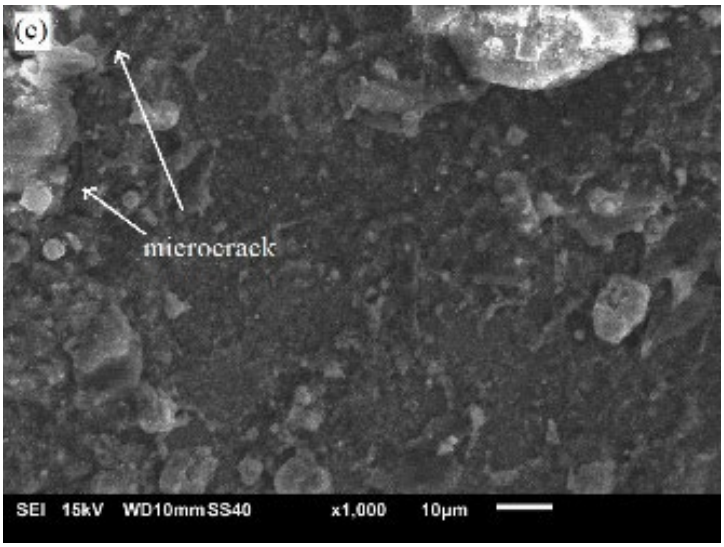

Fig. 9 SEM images of substrates under: (a) low operating conditions, (b) high discharge duration and (c) high powder concentration

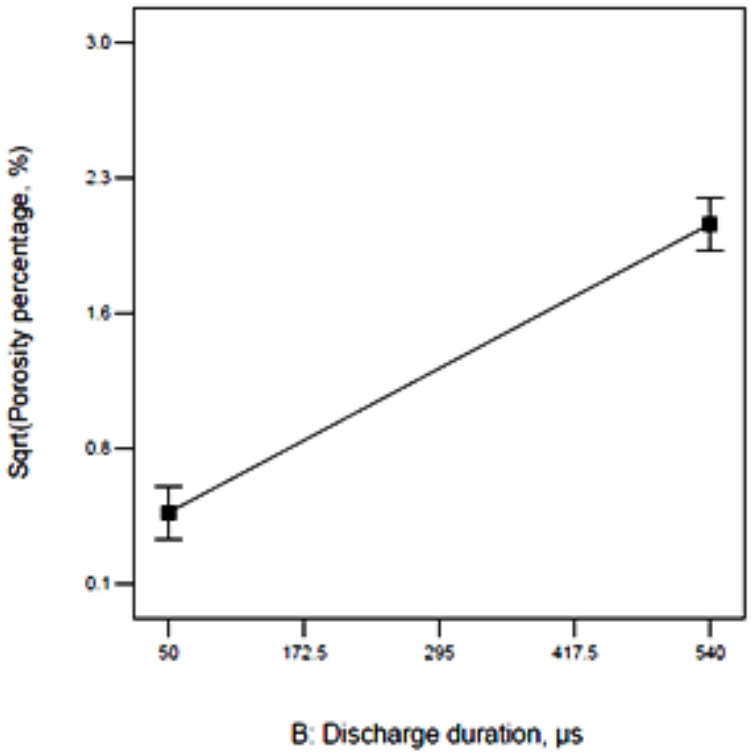

Fig. 10 Graphs of absolute significant parameter of B-discharge duration on the porosity fraction

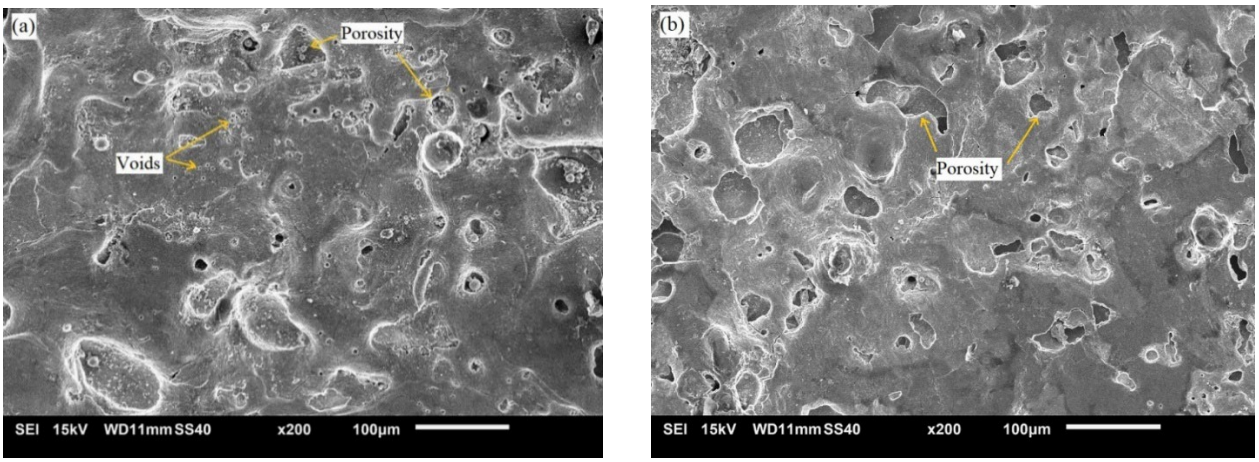

Fig. 11 Surface topography of substrate under high discharge duration with; (a) 0 and (b) 6 g/l of powder concentrations

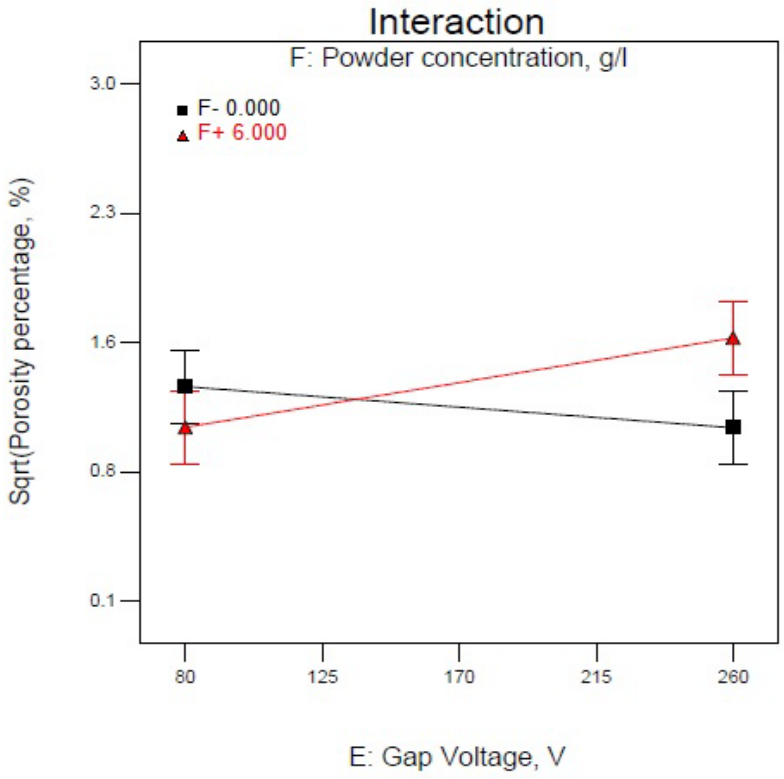

Fig. 12 Graphs of significant EF interaction on the porosity fraction

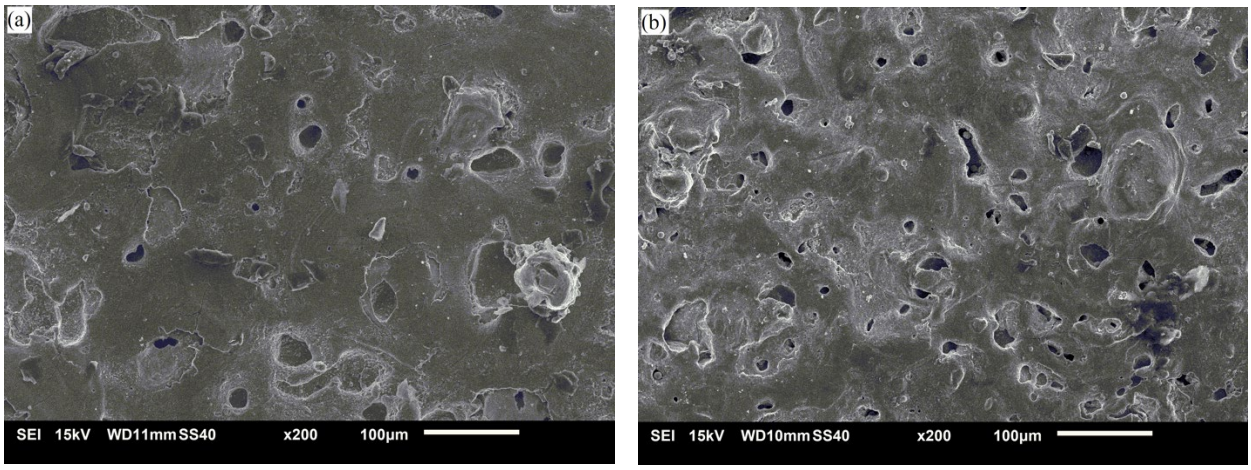

Fig. 13 Surface topography of substrate under high gap voltage with: (a) 0 and (b) 6 g/l of powder concentrations

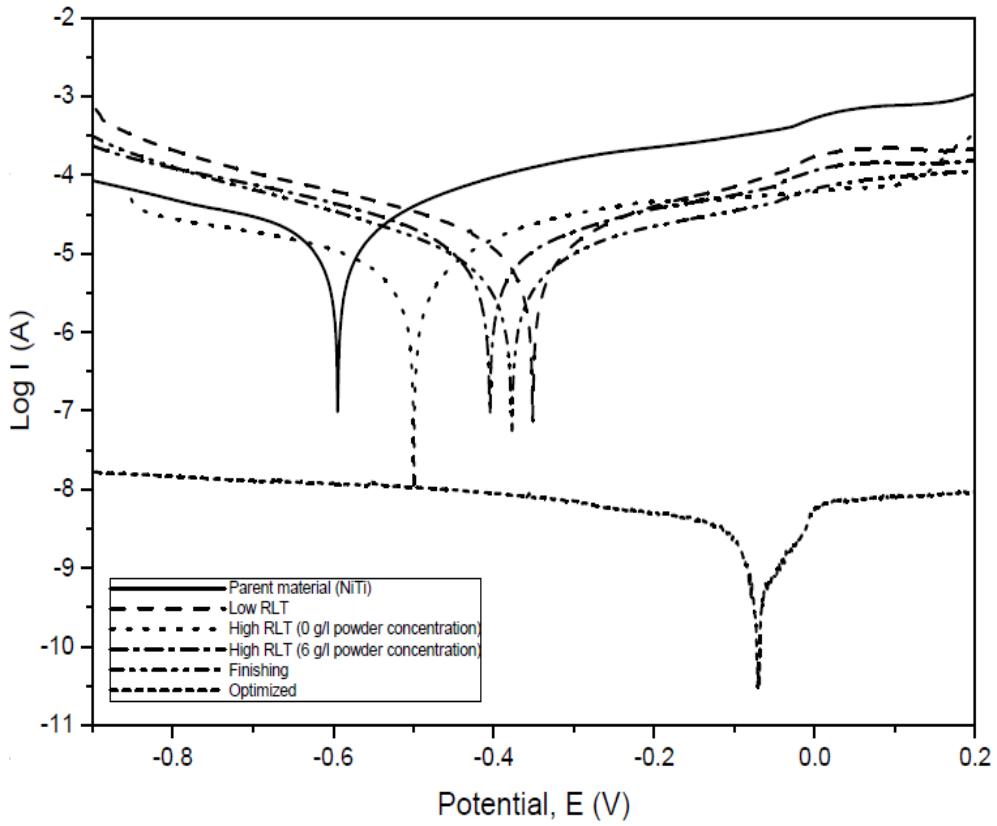

Fig. 14 Potentiodynamic polarization curves of the treated substrates

Table 1 Properties of NiTi SMA

Mechanical properties			
Tensile strength (MPa)	Elongation (%)	Yield strength (MPa)	
850	16	202	
Temperature transformation (°C)			
M_s	M_f	A_s	A_f
-6.02	-27.79	16.14	25.16

Table 2 Parametric conditions

No	Parameters	Unit	Setting value	
			-1	+1
1	Polarity	---	A: straight	B: reverse
2	Discharge duration	µs	50	540
3	Pulse interval	ms	6	8
4	Peak current	amp	3	9
5	Gap voltage	volt	80	260
6	Powder concentration	g/litre	0	6

Table 3 Potentiodynamic polarization results of NiTi substrates in the PBS solution

No	Substrate	I_{corr} (µA/cm²)	E_{corr} (Volts)	Anodic slope, B_a (1/volt)	Cathodic slope, B_c (1/volt)	Polarization resistance, R_p (Ω)	Corrosion rate, (mm/year)
1.	Parent material (NiTi)	253.77	-0.60	1.84	0.88	2890.02	2.95
2.	Low RLT	78.79	-0.35	2.21	1.11	5048.2	0.92
3.	High RLT (0 g/l powder concentration)	106.76	-0.50	-2.42	1.07	4071.20	1.24
4.	High RLT (6 g/l powder concentration	52.42	-0.41	0.93	1.78	7756.50	0.61
5.	Finished	19.97	-0.38	0.68	0.75	7784.50	0.23
6.	Optimized	3.43×10^{-6}	-0.07	3.19	0.34	17.9×10^{6}	8.57×10^{-3}